



# Distributed Hydrological Models

Yangbo Chen

## Contents

1	Introduction .....	414
2	Model Structures .....	415
2.1	Basin Division .....	416
2.2	Terrain Property Data Preparation .....	416
2.3	Flow Network .....	417
2.4	Hydrological Processes .....	417
3	Methodologies for Calculating Hydrological Processes .....	418
3.1	Interception and Evapotranspiration .....	418
3.2	Runoff Formation and Movement .....	419
3.3	Runoff Routing .....	421
4	Parameter Determinations .....	423
4.1	Parameter Classification .....	424
4.2	Scalar Method .....	424
4.3	Automated Parameter Optimization .....	424
5	Case Study .....	425
5.1	Studied Basin and Hydrological Data .....	425
5.2	Terrain Property Data .....	425
5.3	Liuxihe Model Construction .....	426
5.4	Determination of the Initial Parameter Values .....	427
5.5	Automated Parameter Optimization .....	430
5.6	Model Validation .....	431
6	Conclusion .....	434
	References .....	434

---

Y. Chen (✉)

Department of Water Resources and Environment, Sun Yat-sen University, Guangzhou, Guangdong Province, China

e-mail: [eescyb@mail.sysu.edu.cn](mailto:eescyb@mail.sysu.edu.cn)

© Springer-Verlag GmbH Germany, part of Springer Nature 2019

Q. Duan et al. (eds.), *Handbook of Hydrometeorological Ensemble Forecasting*,  
[https://doi.org/10.1007/978-3-642-39925-1\\_23](https://doi.org/10.1007/978-3-642-39925-1_23)

413

---

**Abstract**

Physically based distributed hydrological models (PBDHMs), the development of which has been facilitated by advancements in GIS and remote sensing, meteorology, computer science and engineering, and other related science and engineering disciplines, divide the terrain of a basin into fine-resolution cells and calculate the hydrological processes at both the cell and basin scales. Numerous PBDHMs have been proposed. Because PBDHMs can model hydrological processes at a fine resolution and physically derive model parameters from the properties of the terrain, they have the potential to simulate/predict hydrologic processes more effectively, and they can be employed within ungauged basins. Following a brief review of the development of PBDHMs, this chapter introduces the general structures and methodologies of currently utilized PBDHMs. The basin division method, the sources of terrain property data used to construct PBDHMs, and the flow network delineation method are summarized, and the hydrological processes within watersheds, including interception, evapotranspiration, runoff formation and movement, and runoff routing, are discussed. The methodologies most commonly employed by PBDHMs are then introduced, including those used to calculate the interception, evaporation, runoff formation, and runoff routing. Parameter determination methods are discussed, three of which are introduced in detail: the physically based method, the scalar method, and the automated optimization method. Finally, a case study is presented that demonstrates the entire procedure of constructing a Liuxihe model for a river basin flood simulation/prediction to provide the reader with a complete example of the application of a PBDHM to a real-world problem.

---

**Keywords**

Distributed hydrological model · Hydrological process · Flow network · Terrain property · GIS · Remote sensing · Uncertainty · Parameter optimization · Flood forecasting · Liuxihe model · Particle swarm optimization

---

**1 Introduction**

A distributed hydrological model is a type of hydrological model that divides the terrain of an entire studied basin into numerous cells and then characterizes the hydrological processes, including interception and evapotranspiration, snowmelt, infiltration, and runoff formation and movement at both the cell and basin scales. Distributed hydrological models were modified from lumped hydrological models, which regard the entirety of a basin as uniform, i.e., all of the hydrological processes occur at the basin scale. The development of distributed hydrological models from lumped models was facilitated by advancements in GIS and remote sensing, meteorology, computer sciences and engineering, and other related science and engineering disciplines. Distributed hydrological models are usually physically based, and

thus, they are also known as physically based distributed hydrological models (PBDHMs) (Chen et al. 2011). PBDHMs assign different model parameters to different cells in consideration of terrain property impacts on hydrological processes at the cell scale. Thus, PBDHMs better represent basin characteristics and hydrological processes, and they have the potential to simulate hydrologic responses more effectively (Ambroise et al. 1996). PBDHMs are physically based models, which means that they can physically derive the model parameters from the properties of the terrain. Consequently, there is no need to calibrate the model parameters using long series of observed data, and PBDHMs can be utilized for ungauged basins.

The blueprints for PBDHMs were initially published by Freeze and Harlan (1969), but the first complete PBDHM (i.e., the SHE model) was not published until 1987 (Abbott et al. 1986a, b). Subsequently, due to their rapid development, many PBDHMs have been proposed, including the WATERFLOOD model (Kouwen 1988), VIC model (Xu et al. 1994), DHSVM model (Wigmosta et al. 1994), CASC2D model (Julien et al. 1995), WetSpa model (Wang et al. 1997), GBHM model (Yang et al. 1997), WEP-L model (Jia et al. 2001), Vflo model (Vieux and Vieux 2002), tRIBS model (Vivoni et al. 2004), WEHY model (Kavvas et al. 2004), and the Liuxihe model (Chen et al. 2011).

This chapter, which is divided into four main sections, seeks to introduce the general structures and methodologies of currently utilized PBDHMs by providing a synthesis of typical PBDHMs. Section 2 introduces the model structures (i.e., the methodologies) used to construct typical PBDHMs, including the basin division method, the sources of terrain property data for the model construction, the flow network delineation method, and the hydrological processes considered in most PBDHMs. Section 3 introduces the methods employed by most PBDHMs to calculate those hydrological processes, including interception and evapotranspiration, runoff formation, and runoff routing. Section 4 introduces three of the methods that are used to determine the model parameters employed by most PBDHMs: the physically based method, the scalar method, and the automated parameter optimization method. Section 5 presents a case study that exemplifies the procedure in establishing the Liuxihe model for a river basin flood simulation/prediction to provide the reader with a complete example of how to utilize a PBDHM to solve a real-world scenario. Finally, Sect. 6 concludes this chapter. Owing to page limitations, neither the individual PBDHMs nor the methods employed by the specific PBDHMs are introduced; rather, only the most popular models and methods are discussed. Interested readers are directed to specific publications if they are interested in a specific PBDHM.

---

## 2 Model Structures

The model structure refers to the methodologies used to subdivide basins and calculate the hydrological processes. Different PBDHMs clearly have different model structures.

## 2.1 Basin Division

The first step in the establishment of a PBDHM is to divide the basin into both horizontal and vertical cells. There are two ways to divide a basin into horizontal cells. The first method, which is known as gridded division, divides the basin into grid cells with equivalent dimensions using a gridded digital elevation model (DEM). The second method, which is known as triangular division, divides the basin into triangular cells that have different sizes. There are three advantages of gridded division: the DEM that is used for the terrain division can be easily acquired, the division can be performed automatically, and the code for running the model can be easily operated. The computational requirements for PBDHMs are immense, and thus, executing them on a large computer is necessary. For this reason, gridded division is adopted by most PBDHMs (except for the tRIBS model). Triangular division is advantageous because it considers the local topography when subdividing the terrain, and thus, the number of cells can be reduced compared with the gridded division method. However, as this division cannot be performed automatically, and because some manual operations are required, the division itself cannot be conducted easily. Additionally, since the sizes of the cells are not the same, the code is not as simple as that for gridded division.

The cells are further divided into vertical layers, and a three-layer division method is the most popular. The three layers are known herein as the upper layer, middle layer, and lower layer, respectively, although different models may adopt their own nomenclatures. The upper layer usually extends from the top of the canopy to the land surface, while the middle layer, which is also called the unsaturated zone in some models (i.e., since the soil content in this layer is time-dependent), is usually the layer below the land surface to a particular depth. The lower layer is below the middle layer. Alternative models (e.g., the SHE model) may further subdivide the lower layer into additional zones, but it is usually difficult to practically model multiple lower layers as the necessary data are very difficult to acquire.

In some PBDHMs, the cells are categorized into different types. For example, in the Liuxihe model, the cells are categorized into hillslope cells, river channel cells, and reservoir cells. For different types of cells, alternative calculations are employed for the different hydrological processes.

## 2.2 Terrain Property Data Preparation

After dividing the basin into a grid, the terrain property data, which mainly consist of a DEM, a soil type, and a land use/cover type, must be prepared for every cell. Currently, with the development of satellite remote sensing techniques and joint international efforts, global-scale terrain property data are widely available and can be accessed and downloaded freely via the Internet, which greatly facilitates the development and application of PBDHMs. For example, high-resolution DEMs with resolutions of approximately 90 m by 90 m and 30 m by 30 m can be downloaded from the Shuttle Radar Topography Mission (SRTM) DEM database (Falorni et al.

2005, Sharma and Tiwari 2014), which has proven effective in mountainous basins and has been widely used worldwide. The US Geological Survey (USGS) land use type database (Loveland et al. 1991, 2000) and the Food and Agriculture Organization of the United Nations (FAO) soil type database (<http://www.isric.org>) are popular databases with resolutions of 1000 m by 1000 m, and they can also be downloaded freely. The terrain property data for the example basin given in Sect. 5 were downloaded from these databases and worked well for constructing the model.

### 2.3 Flow Network

In a PBDHM, runoff is first produced in a cell, after which it is routed into adjacent cells until it reaches the basin outlet. The runoff is routed from one cell to the next, which constitutes the runoff flow network for the entire basin, is known as the flow direction.

The D8 flow direction method (O'Callaghan and Mark 1984; Jensen and Domingue 1988) is widely used in PBDHMs to derive a flow network. As there are eight neighboring cells for every cell in a gridded division scheme, the D8 method assumes that there are eight possible flow directions for every cell. These possible flow directions, which represent the direct runoff routing from the center of a cell to the center of a neighboring cell, are labeled East, Southeast, South, Southwest, West, Northwest, North, and Northeast, and they are denoted by one of eight integers: 1, 2, 4, 8, 16, 32, 64, or 128. However, during real-time runoff routing, a cell takes a single flow direction that represents flow to a neighboring cell with the lowest adjacent elevation.

The flow network inclusively determines the runoff routing for the entire basin, and it is further subdivided into hillslope runoff routing and river runoff routing. The runoff routing in a river channel is calculated using the river channel routing method, while the runoff routing on a hillslope is calculated using the hillslope routing method. The methods employed to calculate runoff routing for different models are variable and will be discussed in the next section.

The flow accumulation is usually employed to extract a river channel from a flow network. Given a threshold value for the flow accumulation (e.g., FA0), the flow direction in a cell is regarded as a river channel if the flow accumulation in the cell is larger than FA0. Clearly, the value of FA0 plays a key role in extracting river channels from flow networks, and different FA0 thresholds will result in different river channels. Therefore, during practical modeling endeavors, an extracted river channel should be compared with an available river channel system, and the results should be contrasted with those derived using different FA0 values in order to choose an appropriate FA0 threshold in consideration of trade-offs among the results.

### 2.4 Hydrological Processes

The hydrological processes in PBDHMs are further subdivided into several sub-hydrological processes and can usually be categorized as interception and evapotranspiration, snowmelt, and runoff formation and movement. Runoff

formation processes can be further subdivided into infiltration, surface runoff formation, subsurface runoff formation, and underground runoff formation, while runoff movement is usually divided into hillslope routing and river routing.

### 3 Methodologies for Calculating Hydrological Processes

#### 3.1 Interception and Evapotranspiration

##### 3.1.1 Interception

Falling precipitation will first be intercepted by the vegetation canopy. Specified vegetation types exhibit definitive storage capacities; after this storage capacity is reached, the precipitation will then pass through the canopy layer to the land surface, which is known as the net precipitation. This assumption is widely adopted by PBDHMs, and the storage capacity is usually calculated with the following equation (Dickinson 1984):

$$W_m = K \cdot LAI \quad (1)$$

where  $W_m$  is the canopy storage capacity, LAI is the leaf area index, and K is a constant, which is recommended to be set at 0.2 mm (Xu et al. 1994). The primary purpose of some models is to study flood runoff. Since the volume of interception is considerably small relative to that of the total runoff, interception is usually neglected within such models (e.g., the Vflo and Liuxihe models).

In PBDHMs, the canopy interception is calculated at the cell scale; if there is more than one type of vegetation within a single cell, then the interception quantity is calculated according to each type of vegetation.

##### 3.1.2 Evaporation from the Canopy

Stored water within the canopy is evaporated through canopy evaporation. In PBDHMs, water intercepted by the canopy is believed to evaporate according to a potential evaporation capacity that is determined by the vegetation type.

The canopy evaporation is also calculated at the cell scale. If the PBDHM has a very fine resolution, then only one vegetation type is considered within a single grid cell; however, if the resolution is coarser, then the evaporation must be calculated for each of the several vegetation types and then summed for the grid cell.

##### 3.1.3 Canopy Transpiration

After the intercepted water within the canopy is evaporated, the vegetation will undergo transpiration. Water stored in the soil, i.e., the middle layer, is taken up by the roots of the vegetation and depleted via canopy transpiration. This is a continuous process that partly causes the soil water to change dynamically, which is why the middle layer is also known as the unsaturated zone.

The most common method used to calculate the canopy transpiration in a PBDHM is the Penman-Monteith equation (Monteith 1965; Abbott et al. 1984b):

$$E_a = \frac{R_n \Delta + \frac{QC_p \delta_e}{r_a}}{\lambda \left[ \Delta + \gamma \left( 1 + \frac{r_c}{r_a} \right) \right]} \quad (2)$$

where  $E_a$  is the actual transpiration,  $R_n$  is the net radiation,  $\Delta$  is the rate of increase with temperature of the saturation vapor pressure of water at air temperature,  $Q$  is the density of air,  $r_a$  is the aerodynamic resistance to water vapor transport,  $\lambda$  is the latent heat of the evaporation of water,  $\gamma$  is the psychrometric constant, and  $r_c$  is the canopy resistance to water transport.

As stated above, if the model is primarily utilized for flood forecasting purposes, the canopy transpiration may not be calculated, or it may be calculated simply (e.g., in the Vflo model, the evaporation and transpiration quantities are typically not calculated for flood forecasting). Meanwhile, in the Liuxihe model, a comparatively simple method that requires fewer vegetation and soil property data is employed to calculate the evapotranspiration (Chen et al. 2011) as follows:

$$\begin{aligned} E &= \lambda E_p \text{ if } \theta > \theta_{fc} \\ E &= \lambda E_p \frac{\theta - \theta_w}{\theta_{fc} - \theta_w} \text{ if } \theta_w < \theta \leq \theta_{fc} \\ E &= 0 \text{ if } \theta < \theta_w \end{aligned} \quad (3)$$

where  $E$  is the actual evaporation,  $\theta_{fc}$  is the soil water content under field conditions,  $\theta_w$  is the soil water content under wilting conditions,  $\theta$  is the current soil water content,  $E_p$  is the potential evaporation, and  $\lambda$  is the evaporation coefficient that is determined by the vegetation type. For river and reservoir cells, the evaporation coefficient is 1, while for other vegetation types, it takes a value between 0 and 1.

## 3.2 Runoff Formation and Movement

Precipitation passes through the canopy, reaches the land surface, and then infiltrates into the soil to compensate for the soil water deficit in the middle layer (i.e., the unsaturated zone). Runoff exists in three forms: surface runoff, subsurface runoff, and underground runoff.

### 3.2.1 Infiltration and Surface Runoff Routing

There are two mechanisms that govern infiltration processes. The first is the excess-runoff mechanism that assumes the existence of an infiltration capacity. When the precipitation that reaches the land surface exceeds the infiltration capacity, the precipitation will then infiltrate into the soil at the infiltration capacity to compensate for the soil water deficit, and the surplus precipitation (i.e., exceeding the infiltration capacity) will comprise the surface runoff. The most commonly used method to estimate the infiltration capacity is the Green and Ampt equation, which is written as follows (Rawls et al. 1983; Julien et al. 1995):

$$f = K \left( 1 + \frac{H_f M_d}{F} \right) \quad (4)$$

where  $f$  is the infiltration rate;  $K$  is the hydraulic conductivity;  $H_f$  is the capillary pressure head at the wetting front;  $M_d$  is the soil moisture deficit, which is equal to  $(\theta_e - \theta_i)$ ;  $\theta_e$  is the effective porosity, which is equal to  $(\phi - \theta_r)$ ;  $\phi$  is the initial soil porosity;  $\theta_r$  is the residual saturation;  $\theta_i$  is the initial soil moisture content; and  $F$  is the total infiltration depth.

The second mechanism is the saturation-runoff mechanism, which assumes that the infiltration capacity is sufficiently large inasmuch that all precipitation will infiltrate into the soil before it is saturated, and thus, no surface runoff will be formed. Following the saturation of the soil, a constant infiltration capacity is used to represent the soil, and all precipitation is converted into surface runoff except for the precipitation that infiltrated into the soil according to the constant infiltration capacity.

Surface runoff is routed toward the river outlet in two forms: hillslope runoff routing and river runoff routing. Hillslope runoff routing is the surface runoff that flows along hillslopes before entering a river channel, while river runoff routing is the surface runoff flowing within the river channel. Different methods are employed to calculate these two forms of surface runoff routing, and they will be described in detail in the following subsection.

### 3.2.2 Subsurface Runoff and Movement

Subsurface runoff is the water stored within the middle layer (i.e., the unsaturated zone) and is controlled by infiltration, evapotranspiration, and subsurface runoff flow. In most PBDHMs, only vertical subsurface flow is considered. For example, only vertical flow is assumed in the SHE model, and it is modeled using the one-dimensional Richards equation:

$$C \frac{\partial \psi}{\partial t} = \frac{\partial}{\partial z} \left( K \frac{\partial \psi}{\partial z} \right) + \frac{\partial k}{\partial z} - S \quad (5)$$

where  $\psi$  is the soil moisture tension or pressure head,  $t$  denotes the time,  $z$  is the vertical spatial coordinate (positive upward),  $C$  is the soil water capacity,  $\theta$  is the volumetric water content,  $K(\theta, z)$  is the hydraulic conductivity, and  $S$  is the source/sink term for both the root extraction and soil evaporation.

Some models also consider horizontal subsurface flow when the soil water content is high. For example, in the Liuxihe model, a constant vertical water flow and a horizontal flow are modeled if the water content in the soil layer reaches a minimum value.

### 3.2.3 Underground Runoff and Movement

Water in the lower layer (i.e., the saturated layer) is considered underground runoff. In most PBDHMs, only horizontal flow is considered (e.g., in the SHE model), and each cell is modeled using the nonlinear Boussinesq equation:

$$S \frac{\partial h}{\partial t} = \frac{\partial}{\partial x} \left( K_x H \frac{\partial h}{\partial x} \right) + \frac{\partial}{\partial y} \left( K_y H \frac{\partial h}{\partial y} \right) + R \quad (6)$$

where  $S(x,y)$  is the specific yield;  $h(x,y,t)$  is the phreatic surface level;  $K_x(x,y)$  and  $K_y(x,y)$  are the saturated hydraulic conductivities in the  $x$  and  $y$  directions, respectively;  $H(x,y,t)$  is the saturated thickness;  $t$  denotes the time;  $x$  and  $y$  are the Cartesian coordinates in the horizontal plane; and  $R(x,y,t)$  is the instantaneous vertical recharge into the saturated zone.

Large quantities of data are required to solve the above equation due to its complexity. As a consequence, many PBDHMs do not consider underground runoff in practice, or they simply utilize a lumped underground flow model.

### 3.3 Runoff Routing

#### 3.3.1 Hillslope Routing Methods

Theoretically, runoff flow is governed by the Saint-Venant equations of continuity and momentum with three-dimensional hydrodynamic flow; however, since the Saint-Venant equations are partial differential equations, fully solving these equations with the hydrodynamic method takes an enormous amount of computational time, particularly since the runoff routing must be performed cell-by-cell. Therefore, to ensure the method is practical, the complete Saint-Venant equations must be simplified, after which some effective algorithms are necessary to solve the simplified equations. Two types of simplifications are currently applied in PBDHMs for surface runoff routing. The first type, as is adopted by the SHE model, treats surface runoff flow as a two-dimensional flow; meanwhile, for the second type, all of the other PBDHMs treat surface runoff flow as a one-dimensional flow.

For the SHE model, the two-dimensional flow Saint-Venant equations are written as follows (Abbott et al. 1984b):

$$\frac{\partial h}{\partial t} + \frac{\partial(uh)}{\partial x} + \frac{\partial(vh)}{\partial y} = q \quad (7)$$

$$\frac{\partial h}{\partial x} = S_{0x} - S_{fx} \quad (8)$$

$$\frac{\partial h}{\partial y} = S_{0y} - S_{fy} \quad (9)$$

where  $h(x,y)$  is the local water depth,  $t$  denotes the time,  $x$  and  $y$  are the Cartesian coordinates in the horizontal plane,  $u(x,y)$  and  $v(x,y)$  are the flow velocities in the  $x$  and  $y$  directions,  $q(x,y,t)$  is the net precipitation minus infiltration,  $S_{0x}(x,y)$  and  $S_{0y}(x,y)$  are hillslopes along the  $x$  and  $y$  directions, and  $S_{fx}(x,y)$  and  $S_{fy}(x,y)$  are friction slopes along the  $x$  and  $y$  directions.

In the SHE model, the above equations are solved using the explicit procedure described by Preissmann and Zaoui (1979). In practice, this method is very time

consuming and exhibits a problem with convergence, and thus, it is currently only used in the SHE model.

For all other PBDHMs, surface runoff is treated as a one-dimensional flow along the slope. To greatly reduce the calculation time required, the kinematic wave approximation is employed to solve the equation, which is simplified below:

$$\frac{\partial Q}{\partial x} + L \frac{\partial h}{\partial t} = q \quad (10)$$

$$S_f = S_0 \quad (11)$$

where  $Q$  is the surface flow,  $h$  is the surface flow depth,  $q$  is the lateral flow,  $L$  is the length of the cell,  $S_0$  is the hillslope, and  $S_f$  is the friction slope.

The above equations can be solved using different methods. For example, the finite element algorithm is employed in the Vflo model, while the equation in the Liuxihe model is solved using the Newton iteration algorithm.

Even with the abovementioned simplifications, the surface runoff routing calculation is still very complex and time consuming, and thus, surface runoff routing is neglected in some PBDHMs. Consequently, the produced runoff is regarded as directly flowing into a river channel without runoff routing. Meanwhile, some other PBDHMs employ lumped surface runoff routing methods.

### 3.3.2 River Runoff Routing

River runoff flow is treated as a one-dimensional flow in all PBDHMs, and the diffusive wave approximation is employed to solve the Saint-Venant equations, which are simplified below:

$$\frac{\partial Q}{\partial x} + L \frac{\partial h}{\partial t} = q \quad (12)$$

$$\frac{\partial h}{\partial x} = S_0 - S_f \quad (13)$$

The meanings of the variables in these equations are the same as previously defined. The above equations can also be solved using a variety of methods, but almost all PBDHMs employ the same algorithm to solve for river channel runoff routing with the exception of the SHE model, which employs the MIKE 11 modeling package to conduct full dynamic routing calculations.

In addition to enormous computational requirements, PBDHMs also face challenges during river runoff routing regarding measurements of the shapes of river channels and their cross-sectional sizes. These measurements are particularly difficult or are otherwise impossible to acquire within mountainous watersheds, and thus, PBDHMs are not applicable in many cases due to an absence of essential river channel information. To solve this problem, the river channel shape is assumed to be a trapezoid in the Liuxihe model. Consequently, the river channel cross-sectional size can be measured using two indices for the bottom width and the side slope.

Furthermore, the river channel is divided into virtual sections, and the cross-sectional sizes of the river channel within the same virtual sections are assumed to be equivalent, which greatly simplifies the river channel runoff routing calculation and increases the computational efficiency of the Liuxihe model. In addition, the river channel bottom width is estimated by referencing satellite remote sensing data, and thus, this method can be utilized in regions without field survey data.

---

## 4 Parameter Determinations

Since most model parameters cannot be measured directly, they must be estimated through specific estimation techniques (Laloy et al. 2010; Leta et al. 2015). PBDHMs are physically based models, and thus, their model parameters also possess physical meanings. As a consequence, these parameters can be directly derived from the properties of the terrain. Currently, there are no widely accepted references for deriving these parameters from terrain data; users usually determine the model parameters from alternative references or limited experimental or field results, which are “point” based. This method is herein known as the physically based method. For example, in the Liuxihe model, the parameters are divided into unadjustable and adjustable parameters. The flow direction and slope are two unadjustable parameters that are derived from the DEM, and they remain unchanged. The flow direction is determined using the D8 method introduced above, while the slope is the hill slope along the flow direction that can also be calculated using the DEM. The other parameters are all adjustable parameters that can be adjusted further to improve the model performance. The evaporation capacity is a climate-type parameter, the value of which is set by referencing observations in a watershed and is usually set to 5 mm/day. The evaporation coefficient and roughness are land use-type parameters; the former is a less-sensitive parameter in the Liuxihe model and is usually set to 0.7. The roughness parameter is derived from alternative references or local experimental data. Among the different soil-type parameters, a value of 2.5 is recommended for the parameter *b*, and the soil water content under wilting conditions is set to 30% of the soil water content under field conditions. The values of the other soil-type parameters are calculated using a hydraulic properties calculator for soil water characteristics (Arya and Paris 1981), which calculates the soil water content under saturated and field conditions and the hydraulic conductivity under saturated conditions based on the soil texture, organic matter, gravel content, salinity, and compaction. These calculations can be performed using the program developed by Keith E. Saxton, which can be downloaded from <http://hydrolab.arsusda.gov/soilwater/Index.htm>.

Due to the lack of experimental and field validation research, it has been found that model parameters determined in this manner have high uncertainties in practice. Thus, parameter optimizations are needed to reduce their uncertainties (Gupta et al. 1998; Madsen 2003; Vieux and Moreda 2003; Reed et al. 2004; Smith et al. 2004; Pokhrel et al. 2012; Chen et al. 2016). The scalar method (Vieux et al. 2003), which represents the first effort toward this goal, was proposed to adjust the Vflo model

parameters and was able to improve the model performance. Since this method is performed manually, it is generally very tedious and time consuming. Subsequently, automated parameter optimization methods were developed that improved the efficiencies and capabilities of parameter optimization techniques (Madsen 2003; Shafii and Smedt 2009; Chen et al. 2016).

## 4.1 Parameter Classification

The parameter values in PBDHMs are related to terrain properties, including the topography, soil type, and vegetation type, and thus, these values can be determined through the properties of the terrain (Chen et al. 2016). The model parameters of all PBDHMs are usually classified into one of four different types: climate-related parameters, topography-related parameters, vegetation (land use)-related parameters, and soil-related parameters. With this classification, the parameters in different cells will have the same values if they have the same terrain properties, and thus, they can be determined using a physically based method.

## 4.2 Scalar Method

The scalar method was first utilized for the Vflo model (Vieux et al. 2003). In the scalar method, every parameter value that is derived using a physically based method is manually adjusted with a factor or a multiplier (scalar). The scalars for the same parameter categories among different cells are taken to have the same values, so only a few parameters must be adjusted. The scalar method is simple, but it must be performed manually, and it is consequently tedious and time consuming. However, it has been proven capable of improving the model performance.

## 4.3 Automated Parameter Optimization

For the SHE model, an automatic parameter optimization method using a shuffled complex evolution (SCE) algorithm (Duan et al. 1994) was employed to simulate the catchment runoff (Madsen 2003) in consideration of two objectives: fitting the surface runoff at the catchment outlet and minimizing the error in the simulated underground water level at different wells. To simulate the runoff processes within a medium-sized catchment with the WetSpa model, a multi-objective genetic algorithm was used to optimize the model parameters (Shafii and Smedt 2009). An automated parameter optimization method based on a particle swarm optimization (PSO) algorithm was proposed for the Liuxihe model and was found to be effective (Chen et al. 2016). The PSO algorithm has three steps. The first step is to classify all of the parameters into a few independent parameters (i.e., which will subsequently be optimized) using the same classification method as described above. The second

step is to initialize and normalize the parameters. The parameter initialization is employed to derive the initial model parameter values using the physically based method described above. Then, the parameters are normalized with their initial values as follows:

$$X_i = X'_i/X_{i0} \quad (14)$$

where  $X'_i$  is the original value of a parameter  $i$ ,  $x_{i0}$  is the initial value of a parameter  $i$ , and  $x_i$  is the normalized value of a parameter  $i$ . Every parameter becomes unit-less variable during the normalization process.

The third step is to automatically optimize the independent parameters using an optimization algorithm (i.e., PSO algorithm). The objective function for the optimization algorithm minimizes the peak flow relative error of the catchment discharge at the outlet.

To reduce the computational cost for a large watershed, the parameters sensitive to the model performance may be identified first, after which only relatively sensitive parameters are optimized.

---

## 5 Case Study

In this section, a case study is introduced that employs the Liuxihe model to simulate the flood processes of a river basin. The purpose of this case study is to demonstrate the procedure for constructing a PBDHM to simulate/predict the hydrological processes in a river basin; the procedure for which is the same for other PBDHMs.

### 5.1 Studied Basin and Hydrological Data

The studied basin is the Taiping Watershed, which is a second-order tributary of the Ganjiang River Basin in Jiangxi Province. The Taiping Watershed is 51.6 km long with a drainage area of 445 km<sup>2</sup>. It is a mountainous watershed with frequent flash flooding events. Figure 1 displays a sketched map of the Taiping Watershed.

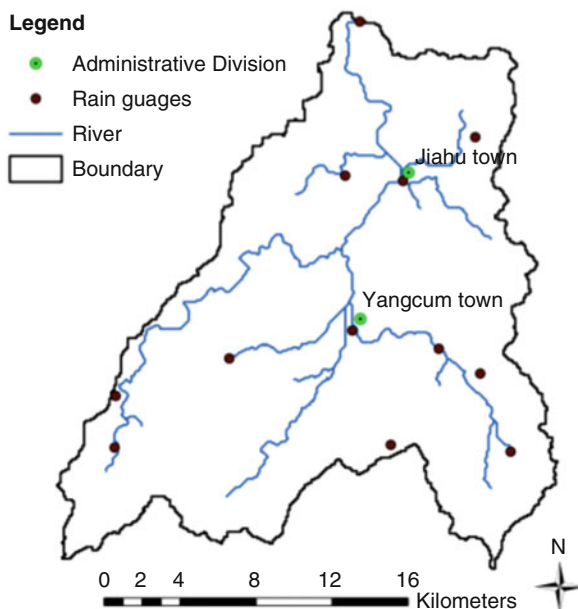
There are 12 rain gauges installed throughout the watershed that automatically collect precipitation. One river gauge is installed at the outlet of the watershed, and it is capable of measuring the discharge continuously. The locations of the rain gauges and river gauge are shown in Fig. 1.

Hydrological data of six flood events observed over the past years, including precipitation and river discharge data, have been collected for this case study.

### 5.2 Terrain Property Data

The terrain property data used for the construction of the Liuxihe model in this case study constitute a DEM in addition to land use types and soil types. These data for the

**Fig. 1** Sketched map of the Taiping Watershed



studied watershed were downloaded from open access databases. The DEM was downloaded from the SRTM database, the land use type data were downloaded from the USGS land cover database, and the soil type data were downloaded from <http://www.isric.org>. The downloaded DEM has a spatial resolution of 90 m by 90 m, but the other two datasets have spatial resolutions of 1000 m by 1000 m. Consequently, they are rescaled to a spatial resolution of 90 m by 90 m. Figure 2 exhibits the terrain property data (i.e., the DEM, land use types, and soil types) of the Taiping Watershed.

### 5.3 Liuxihe Model Construction

To construct the Liuxihe model for the studied watershed, the whole basin of the Taiping Watershed is divided into 55,221 grid cells using the DEM with a grid cell size of 90 m by 90 m (as previously prepared), after which the grid cells are categorized into reservoir cells, river channel cells, and hillslope cells. As there are no significant reservoirs, no reservoir cells are derived during this process.

In this study, different FA0 thresholds are used to derive the river channel cells, the results of which are shown in Fig. 3.

To compare the results of this process with the natural river system of the Taiping Watershed, and to make it possible to estimate the river cross-sectional size using remote sensing data, a third-order river system is adopted. With this division, 1133 river channel cells and 54,088 hillslope cells are produced. Furthermore, 12 nodes are established within the Taiping Watershed, and the river channel system is divided

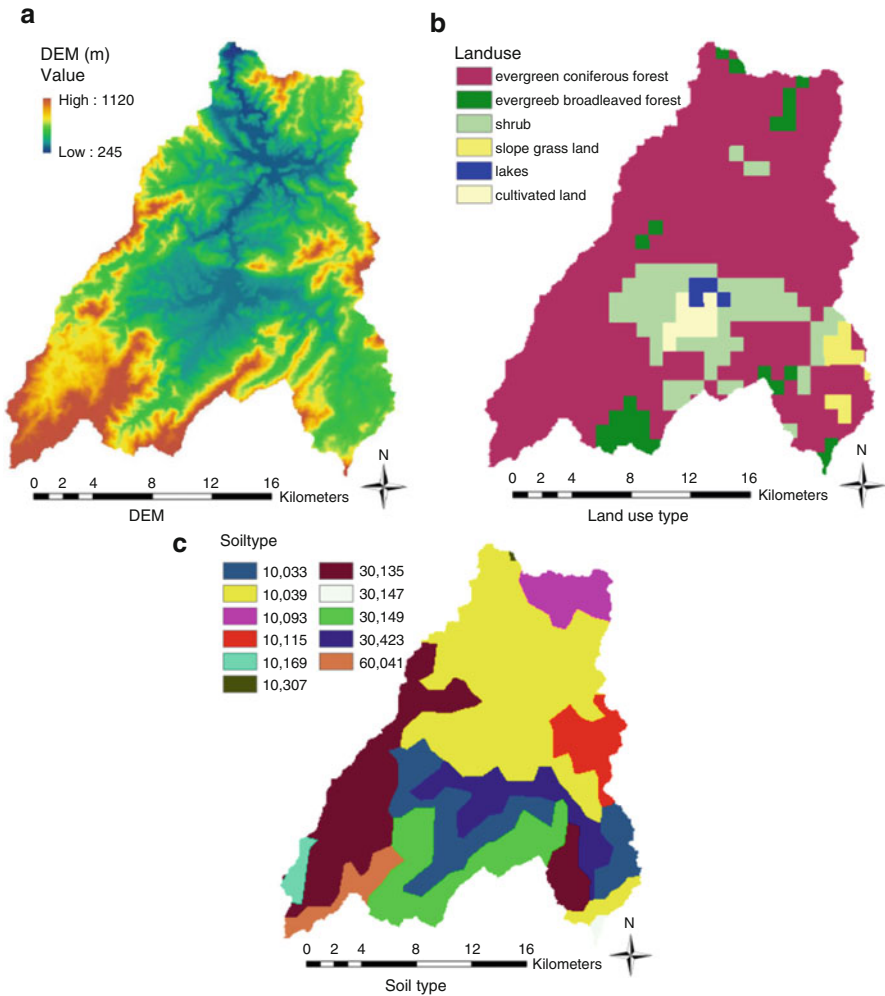


**Fig. 2** Property data of the Taiping Watershed. (a) DEM. (b) Land use type. (c) Soil type

into 29 virtual sections, the cross-sectional sizes of which are estimated through a reference with satellite remote sensing imagery. The Liuxihe model structure of the Taiping Watershed is shown in Fig. 4.

### 5.4 Determination of the Initial Parameter Values

Based on the DEM shown in Fig. 2a, the flow directions and slopes of all of the cells are derived and are shown in Figs. 5 and 6, respectively.

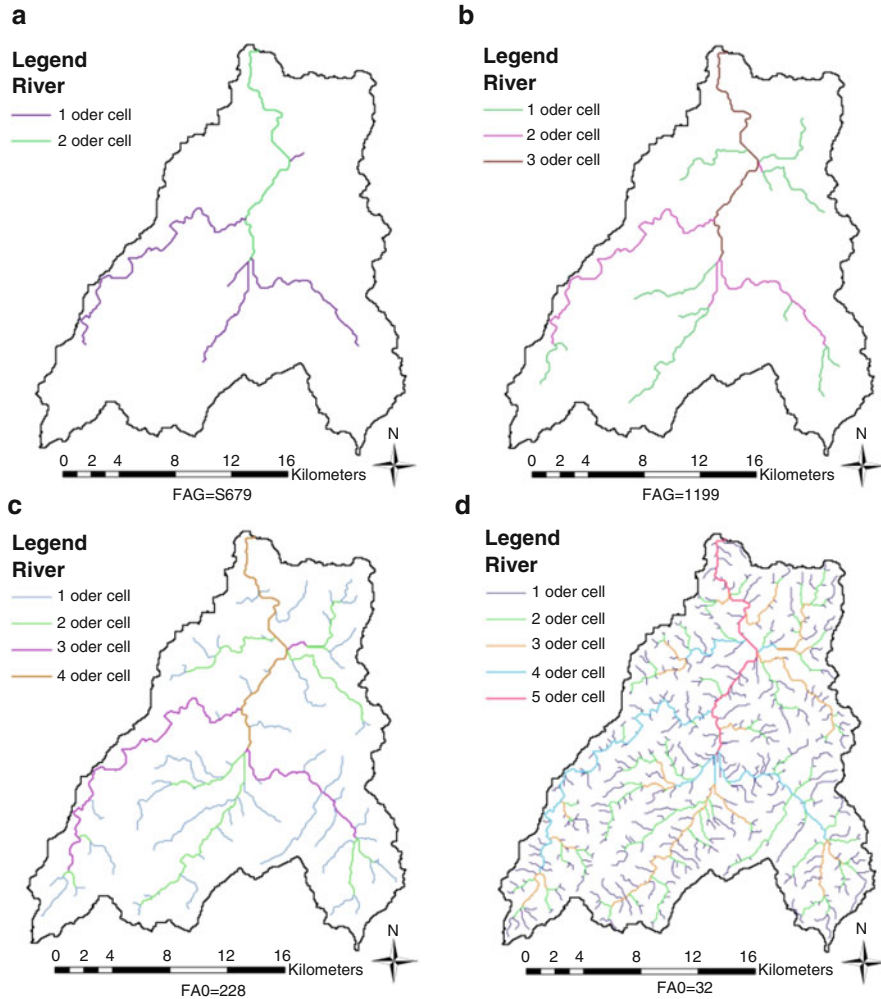


**Fig. 3** River cells classification with different FA0 thresholds. (a) FA0=S679. (b) FA0 = 1199. (c) FA0 = 228. (d) FA0 = 32

The initial value of the evaporation capacity is set to 5 mm/day, and the initial value of the evaporation coefficient is set to 0.7. Meanwhile, the initial value of the roughness is derived based on a reference (Wang et al. 1997). The initial values of the parameters are listed in Table 1.

For the soil-type parameters, the variable  $b$  is set at a value of 2.5, and the soil water content under wilting conditions is taken as 30% of the soil water content under field conditions. The initial values of the soil water content under saturated and field conditions and the hydraulic conductivity under saturated conditions are determined using Keith E. Saxton's simulator based on the soil texture, organic matter,

**Fig. 4** Liuxihe model structure of the Taiping Watershed

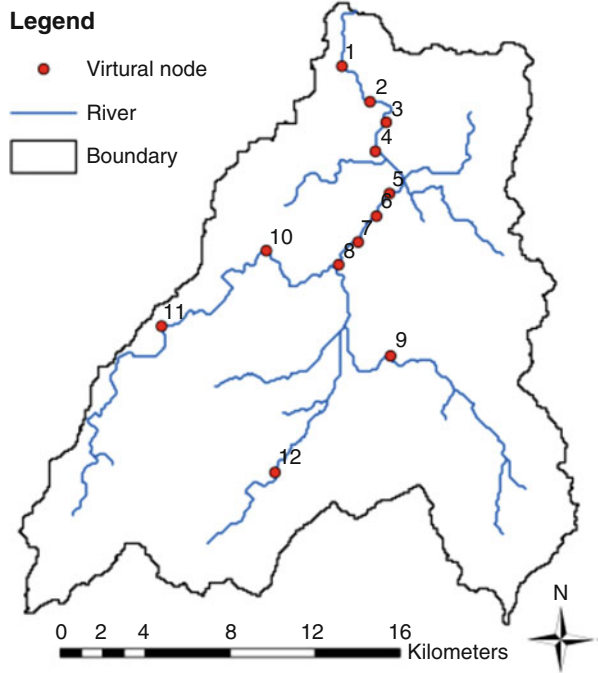


**Fig. 5** Flow direction of the Taiping Watershed

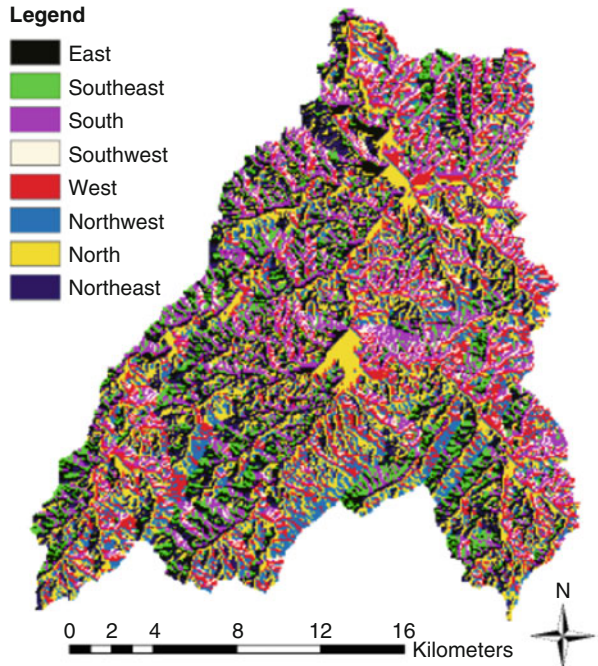


**Fig. 6** Slope of the Taiping Watershed

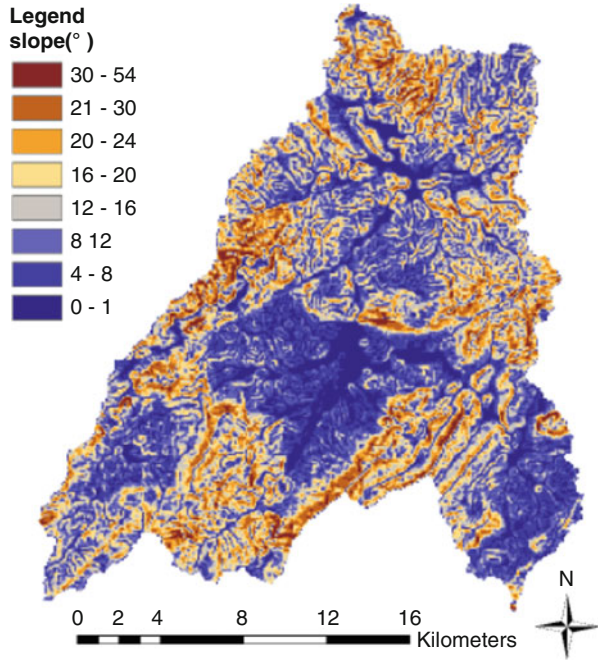


**Table 1** Initial values of the land use-type parameters

ID	Name	Evaporation coefficient	Roughness coefficient
2	Evergreen coniferous forest	0.7	0.4
3	Evergreen broad-leaved forest	0.7	0.6
5	Shrub	0.7	0.4
8	Slope grassland	0.7	0.2
10	Lakes	0.7	0.045
15	Cultivated land	0.7	0.15

gravel content, salinity, and compaction of the soil type. These parameter initial values are listed in Table 2.

### 5.5 Automated Parameter Optimization

The flood event flood2006071409 is used to automatically optimize the model parameters with the initial values, and the particle number used is 20. Figure 7 shows both the objective and parameter evolution processes of the parameter optimization.

**Table 2** Initial values of soil-type parameters

Soil type	Thickness (mm)	Water content at saturated conditions	Water content at field conditions	Hydraulic conductivity at saturated conditions (mm/h)	b
CN10033	1000	0.466	0.354	3.5	2.5
CN10039	600	0.515	0.422	1.95	2.5
CN10093	1000	0.454	0.144	74.49	2.5
CN10115	700	0.5	0.377	4.89	2.5
CN10169	1000	0.438	0.192	35.15	2.5
CN10307	1000	0.451	0.315	6.28	2.5
CN30135	1000	0.435	0.207	28.33	2.5
CN30147	1000	0.443	0.262	14.88	2.5
CN30149	1300	0.429	0.211	24.13	2.5
CN30423	670	0.446	0.24	21.87	2.5
CN60041	870	0.511	0.451	0.51	2.5

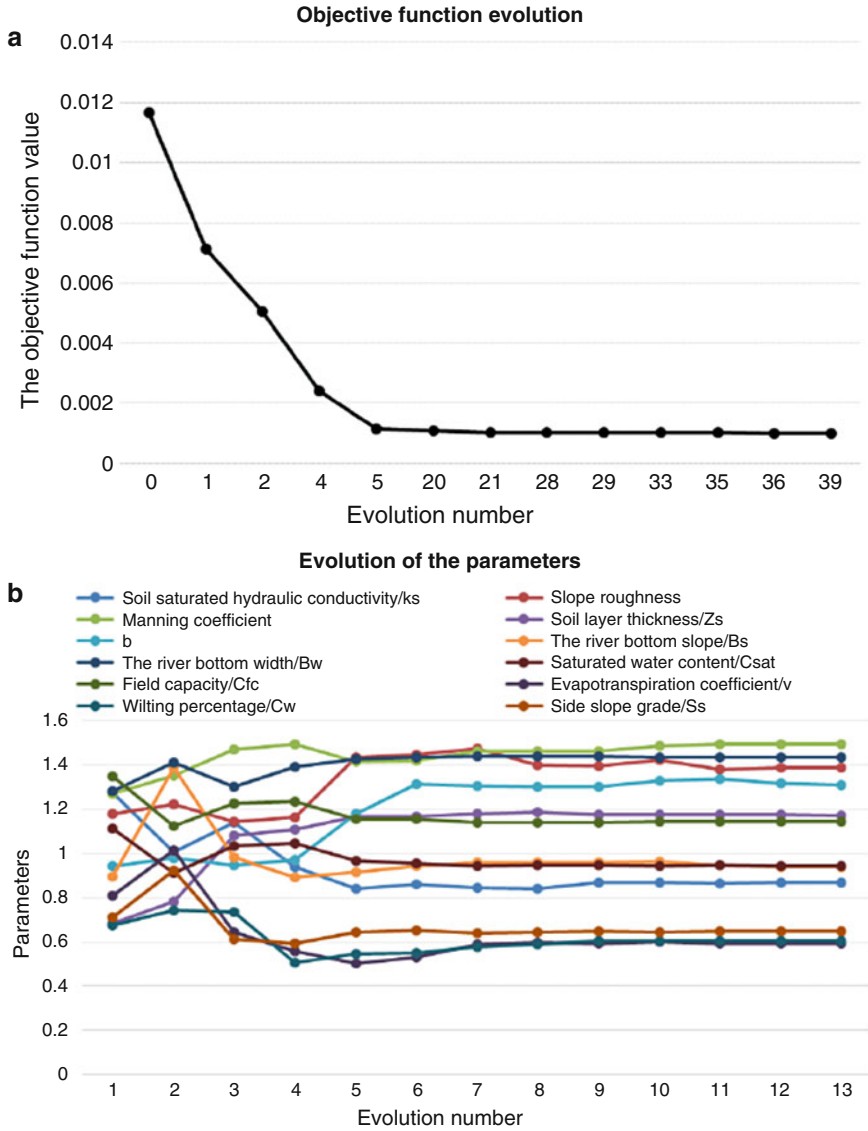
During the evolution process, the objective function rapidly decreases and converges to its optimal value (Fig. 7). After only 5 evolutions, most of the parameters nearly converged to their optimal values; after 12 evolutions, most of the parameters had converged to their optimal values. These results demonstrate that the PSO algorithm exhibits effective convergence capabilities.

Figure 7 also shows that the optimal parameter values of several of the parameters are quite different from the initial parameters, while those of others are relatively unchanged, which implies that the initial model parameters determined using the physically deriving method possess high uncertainties. A parameter optimization algorithm could reduce these uncertainties.

## 5.6 Model Validation

The other observed flood events of the Taiping Watershed are simulated using the model with the parameters that were optimized above to validate the model performance for flood forecasting. To analyze the effects of the parameter optimization on the model performance improvement, Fig. 8 shows three of the simulated hydrographs.

These results reveal that the model with initial parameter values is unable to simulate the observed flood events satisfactorily, i.e., the uncertainties are high. In addition, the simulated hydrographs with the optimized model parameters fit the observed hydrographs well, particularly with regard to the simulated peak flow. These results imply that the parameter uncertainties have been reduced through the model parameter optimization.



**Fig. 7** The evolution processes of the parameter optimization. (a) Objective function evolution. (b) Evolution of the parameters

The above results suggest that using a PSO parameter optimization algorithm can improve the Liuxihe model performance for watershed flood forecasting in the Taiping Watershed and that optimizing the parameters of the Liuxihe model is necessary.

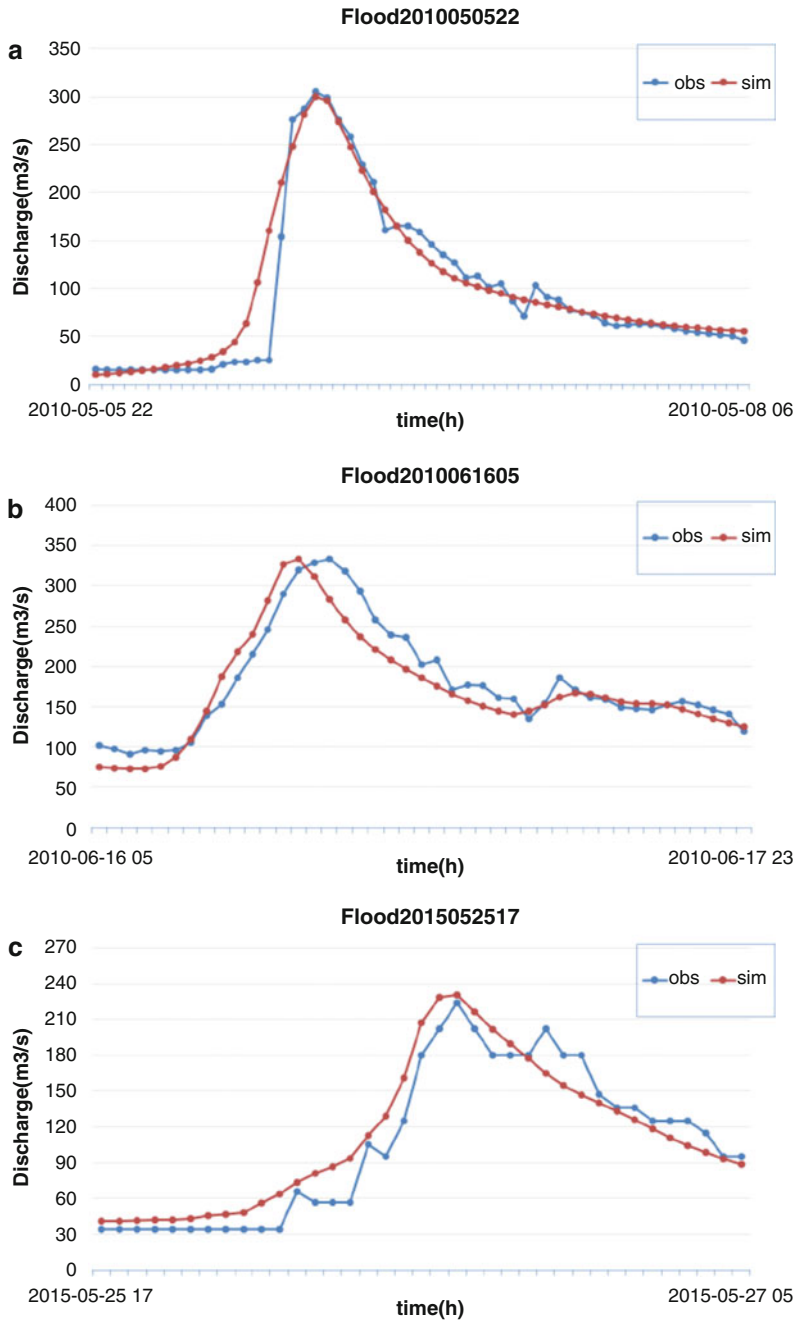


**Fig. 8** Simulated flood events with optimized model parameters. (a) Flood2010050522. (b) Flood2010061605. (c) Flood2015052517

## 6 Conclusion

This chapter introduced the general structures and methodologies of currently employed PBDHMs, and a case study of a watershed in China was presented using the Liuxihe model to demonstrate the complete procedure of constructing a PBDHM for a river basin flood simulation/prediction experiment. The following conclusions can be summarized:

1. A number of PBDHMs have been proposed, and many successful applications of these models have been reported. Scientifically sound PBDHM structures and methodologies have been presented and implemented to satisfy the requirements of these applications. New PBDHMs are not urgently needed, but in order to improve the accuracies of existing PBDHMs, new algorithms for multiple hydrological processes, including infiltration and runoff routing, must be developed based on the advancement of hydrological principle research.
2. Data for the construction of PBDHMs with global coverage are widely available and can be accessed and freely downloaded via the Internet. These data could be satisfactorily utilized to construct PBDHMs for both scientific studies and real-time applications, particularly in mountainous watersheds.
3. Model uncertainties are still high presently, particularly with regard to the determinations of parameters that require high hydrological process simulation/prediction accuracies, e.g., for flood simulation/forecasting applications. Parameter optimization methods, which are necessary for applications requiring high accuracies, have been proposed, and they have proven very useful in improving the model performances. Validation studies in this field still need to be strengthened.
4. Algorithms with higher computational efficiencies still need to be explored. Furthermore, the development of standardized software tools is urgent, and public infrastructures, which could be shared by general users to test new PBDHMs for both scientific studies and real-time applications, should be established.

---

## References

- M.B. Abbott et al., An introduction to the European hydrologic system-system hydrologue European, 'SHE', a: history and philosophy of a physically-based, distributed modelling system. *J. Hydrol.* **87**, 45–59 (1986a)
- M.B. Abbott et al., An introduction to the European hydrologic system-system hydrologue European, 'SHE', b: structure of a physically based, distributed modeling system. *J. Hydrol.* **87**, 61–77 (1986b)
- B. Ambrose, K. Beven, J. Freer, Toward a generalization of the TOPMODEL concepts: topographic indices of hydrologic similarity. *Water Resour. Res.* **32**, 2135–2145 (1996)
- L.M. Arya, J.F. Paris, An empirical model to predict the soil moisture characteristic from particle-size distribution and bulk density data. *Soil Sci. Soc. Am. J.* **45**, 1023–1030 (1981)
- Y. Chen, Q.W. Ren, F.H. Huang, H.J. Xu, I. Cluckie, Liuxihe model and its modeling to river basin flood. *J. Hydrol. Eng.* **16**, 33–50 (2011)
- Y. Chen, J. Li, H. Xu, Improving flood forecasting capability of physically based distributed hydrological model by parameter optimization. *Hydrol. Earth Syst. Sci.* **20**, 375–392 (2016)

- Dickinson, R. E., Modelling evapotranspiration for three-dimensional global climate models, in *Climate Processes and Climate Sensitivity*, Geophys. Monogr. Ser., ed. J. E. Hansen, T. Takahashi, vol. 29 (AGU, Washington, DC, 1984)
- Q. Duan, S. Sorooshian, V.K. Gupta, Optimal use of the SCE-UA global optimization method for calibrating watershed models. *J. Hydrol.* **158**, 265–284 (1994)
- G. Falorni, V. Teles, E.R. Vivoni, R.L. Bras, K.S. Amaratunga, Analysis and characterization of the vertical accuracy of digital elevation models from the Shuttle Radar Topography Mission. *J. Geophys. Res. F: Earth Surf.* **110**(2), F02005 (2005)
- R.A. Freeze, R.L. Harlan, Blueprint for a physically-based, digitally simulated, hydrologic response model. *J. Hydrol.* **9**, 237–258 (1969)
- R.B. Grayson, I.D. Moore, T.A. McMahon, Physically based hydrologic modeling: 1.A terrain-based model for investigative purposes. *Water Resour. Res.* **28**, 2639–2658 (1992)
- H.V. Gupta, S. Sorooshian, P.O. Yapo, Toward improved calibration of hydrological models: multiple and non-commensurable measures of information. *Water Resour. Res.* **34**(4), 751–763 (1998)
- S.K. Jensen, J.O. Domingue, Extracting topographic structure from digital elevation data for geographic information system analysis. *Photogramm. Eng. Remote Sens.* **54**(11), 1593–1600 (1988)
- Y. Jia, G. Ni, Y. Kawahara, Development of WEP model and its application to an urban watershed. *Hydrol. Process.* **15**, 2175–2194 (2001)
- P.Y. Julien, B. Saghafian, F.L. Ogden, Raster-based hydrologic modeling of spatially- varied surface runoff. *Water Resour. Bull.* **31**, 523–536 (1995)
- M. Kavvas, Z. Chen, C. Dogrul, J. Yoon, N. Ohara, L. Liang, H. Aksoy, M. Anderson, J. Yoshitani, K. Fukami, T. Matsuura, Watershed environmental hydrology (WEHY) model based on upscaled conservation equations: hydrologic module. *J. Hydrol. Eng.* **6**(450), 450–464 (2004). [https://doi.org/10.1061/\(ASCE\)1084-0699\(2004\)9](https://doi.org/10.1061/(ASCE)1084-0699(2004)9)
- N. Kouwen, WATFLOOD: a micro-computer based flood forecasting system based on real-time weather radar. *Can. Water Resour. J.* **13**, 62–77 (1988)
- E. Laloy, D. Fusbender, C.L. Bielders, Parameter optimization and uncertainty analysis for plot-scale continuous modeling of runoff using a formal Bayesian approach. *J. Hydrol.* **380**(1–2), 82–93 (2010)
- O.T. Leta, J. Nossent, C. Velez, N.K. Shrestha, A. Griensven, W. Bauwens, Assessment of the different sources of uncertainty in a SWAT model of the River Senne (Belgium). *Environ. Model. Softw.* **68**, 129–146 (2015)
- L. Xu, D.P. Lettenmaier, E.F. Wood, S.J. Burges, A simple hydrologically based model of land surface water and energy fluxes for general circulation models. *J. Geophys. Res.* **99**, 14415–14428 (1994)
- T.R. Loveland, J.W. Merchant, D.O. Ohlen, J.F. Brown, Development of a land cover characteristics data base for the conterminous U.S. *Photogramm. Eng. Remote. Sens.* **57**(11), 1453–1463 (1991)
- T.R. Loveland, B.C. Reed, J.F. Brown, D.O. Ohlen, J. Zhu, L. Yang, J.W. Merchant, Development of a global land cover characteristics database and IGBP DISCover from 1km AVHRR data. *Int. J. Remote Sens.* **21**(6–7), 1303–1330 (2000)
- H. Madsen, Parameter estimation in distributed hydrological catchment modelling using automatic calibration with multiple objectives. *Adv. Water Resour.* **26**, 205–216 (2003)
- J. L. Monteith, Evaporation and environment, in *The State and Movement of Water in Living Organisms. Proceedings of 15th Symposium Society for Experimental Biology, Swansea* (Cambridge University Press, London, 1965)
- J. O’Callaghan, D.M. Mark, The extraction of drainage networks from digital elevation data. *Comput. Vis. Graph. Image Process* **28**(3), 323–344 (1984)
- P. Pokhrel, K.K. Yilmaz, H.V. Gupta, Multiple-criteria calibration of a distributed watershed model using spatial regularization and response signatures. *J. Hydrol.* **418–419**, 49–60 (2012)
- A. Preissmann, J. Zaoui, Le Module “coulement de surface” du Systeme Hydrologique European (SHE), in *Proceedings of 18th Congress International Association for Hydraulic Research, Cagliari*, 5 (1979), pp. 193–199
- W.J. Rawls, D.L. Brakensiek, N. Miller, Green-Ampt infiltration parameters from soils data. *J. Hydraul. Eng. ASCE* **109**(1), 62–70 (1983)

- S. Reed, V. Koren, M. Smith, Z. Zhang, F. Moreda, D.-J. Seo, DMIP participants: overall distributed model intercomparison project results. *J. Hydrol.* **298**(1–4), 27–60 (2004)
- M. Shafii, F.D. Smedt, Multi-objective calibration of a distributed hydrological model (WetSpa) using a genetic algorithm. *Hydrol. Earth Syst. Sci.* **13**, 2137–2149 (2009)
- A. Sharma, K.N. Tiwari, A comparative appraisal of hydrological behavior of SRTM DEM at catchment level. *J. Hydrol.* **519**, 1394–1404 (2014)
- M.B. Smith, D.-J. Seo, V.I. Koren, S. Reed, Z. Zhang, Q.-Y. Duan, S. Cong, F. Moreda, R. Anderson, The distributed model intercomparison project (DMIP): motivation and experiment design. *J. Hydrol.* **298**(1–4), 4–26 (2004)
- B.E. Vieux, F.G. Moreda, Ordered physics-based parameter adjustment of a distributed model, in *Advances in Calibration of Watershed Models*, Water Science and Application Series, ed. by Q. Duan, S. Sorooshian, H.V. Gupta, A.N. Rousseau, R. Turcotte, vol. 6 (American Geophysical Union, Washington, DC, 2003), pp. 267–281. ISBN:0-87590-335-X (Chapter 20)
- B. E. Vieux, J. E. Vieux, Vflo™: a real-time distributed hydrologic model[A], in *Proceedings of the 2nd Federal Interagency Hydrologic Modeling Conference*. 28 July–1 Aug, Las Vegas, Nevada. Abstract and paper on CD-ROM 2002
- E.R. Vivoni, V.Y. Ivanov, R.L. Bras, D. Entekhabi, Generation of triangulated irregular networks based on hydrological similarity. *J. Hydrol. Eng.* **9**(4), 288–302 (2004)
- Z. Wang, O. Batelaan, F. De Smedt, A distributed model for water and energy transfer between soil, plants and atmosphere (WetSpa). *J. Phys. Chem. Earth* **21**, 189–193 (1997)
- M.S. Wigmosta, L.W. Vai, D.P. Lettenmaier, A distributed hydrology-vegetation model for complex terrain. *Water Resour. Res.* **30**, 1665–1669 (1994)
- D. Yang, S. Herath, K. Musiak, Development of a geomorphologic properties extracted from DEMs for hydrologic modeling. *Ann. J. Hydraul. Eng. JSCE* **47**, 49–65 (1997)